Check for updates

*Journal of Applied Polymer Science*

WILEY

Applied Polymer SCIENCE

RESEARCH ARTICLE OPEN ACCESS

# Effects of Ground Rubber Loading on Rubber Compounds Studied by the Hyphenated Rheo-NMR and the Palierne Model

Tim Schülein[1,2] | Sarah L. Palloks[1] | Stefan A. Frosch[2] | Johannes Krückel[2] | Volker Herrmann[2] | Manfred Wilhelm[1]

[1]Institute for Chemical Technology and Polymer Chemistry, Karlsruhe Institute of Technology (KIT), Karlsruhe, Germany | [2]Faculty of Plastics Engineering and Surveying, Technical University of Applied Sciences Würzburg-Schweinfurt (THWS), Würzburg, Germany

**Correspondence:** Manfred Wilhelm (manfred.wilhelm@kit.edu)

**Received:** 6 February 2026 | **Revised:** 8 June 2026 | **Accepted:** 2 July 2026

**Keywords:** Palierne model on rubber compounds | rheology | Rheo-NMR | rubber recycling | vulcanization

## ABSTRACT

This article investigates the effect of ground rubber (GR) loading of rubber compounds using the unique hyphenated Rheo-NMR setup. This setup is used to quantify the effects on the rheological behavior as an emulsion-like blend as well as of the further vulcanization of the GR particle due to sulfur diffusion. The GR as a sustainable component of rubber compounds affects engineering properties. This can be explained by the diffusion of free sulfur from the rubber matrix into the GR particles, resulting in a change in cross-link density (CLD) in the matrix and the GR particles. Another effect that occurs is the emulsion-like blend of GR particles within the rubber matrix describable by adequate constitutive emulsion models. Rubber compounds of styrene-butadiene rubber (SBR) and natural rubber (NR) were used both for the rubber matrix and the self-produced GR. The predictions by the Palierne model describe the rheology with a deviation of up to 15%. NMR results of the GR particle show an increase of 100% in CLD for NR, while SBR shows a decrease of around 13%. Such results have not covered in the literature so far and are of great importance to optimize recycling of rubber materials.

## 1 | Introduction

More than three million tons of passenger car and truck tires are accumulated every year in the European Union after their use [1]. Worldwide, the amount is assumed to be 10 times higher [2]. To advance toward a circular economy, recycling is essential. A potential method is the incorporation of ground rubber (GR) (particle size ranges from 0.2 to 2 mm) into rubber compounds prior to vulcanization [3–7].

The incorporation of GR particles deteriorates the properties of the final product, for example, tensile strength, compared to formulations without GR particles [5, 8]. This can be explained by both emulsion-like blend of the GR particles in the rubber matrix and a change in CLD in the rubber matrix and GR particles due to sulfur diffusion, as shown in Figure 1.

### 1.1 | Sulfur Diffusion From Matrix Into GR Particle

The effect of sulfur diffusion from the matrix into the GR particle originates from free, non-covalently bound sulfur ($S_8$) in the matrix. This diffusion happens during mixing, storage, and vulcanization of the rubber compound. It occurs because $S_8$ sulfur in the rubber matrix is free and mobile, while sulfur in the already vulcanized GR particles is predominantly covalently bound to the polymer chains. Therefore, there is a difference in the chemical potential of free sulfur. The $S_8$ diffusion lowers the overall sulfur concentration in the rubber matrix with a certain gradient and raises it in the GR particles. It is evident that higher amounts of sulfur lead to a higher cross-link density (CLD) during vulcanization [5, 9–11]. Therefore, diffusion of free $S_8$ sulfur leads to an increase in the CLD in the GR particles and to a lower CLD in the

This is an open access article under the terms of the Creative Commons Attribution License, which permits use, distribution and reproduction in any medium, provided the original work is properly cited.

© 2026 The Author(s). *Journal of Applied Polymer Science* published by Wiley Periodicals LLC.

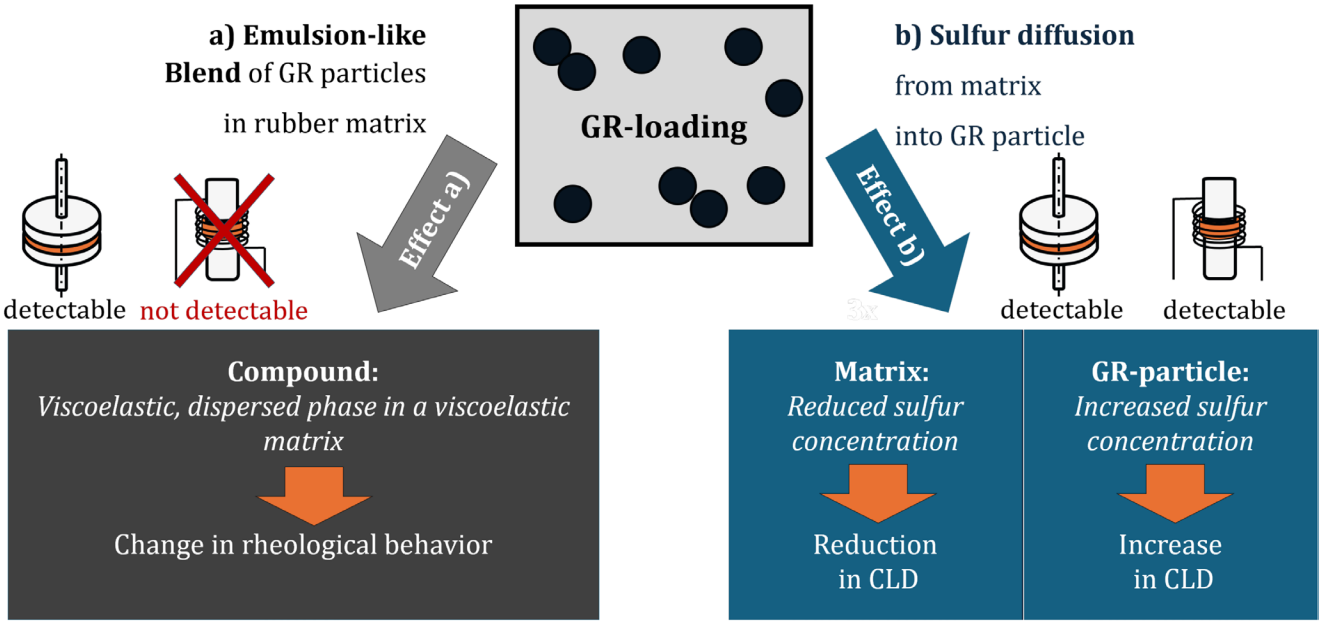


**FIGURE 1** | Effects of GR loading on the vulcanization behavior measured by Rheology and TD-NMR. The effect of the emulsion-like blend of GR particles in the rubber matrix can only be measured by rheology, while the change in CLD due to sulfur diffusion can be measured by both rheology and TD-NMR. [Color figure can be viewed at wileyonlinelibrary.com]

rubber matrix material than intended [10]. Additionally, diffusion of accelerators from the GR particles into the rubber matrix alters the free sulfur-to-accelerator ratio in both phases [9].

### 1.2 | Emulsion-Like Blends of GR Particles in the Rubber Matrix

Another concern encountered when incorporating GR particles in rubber compounds is a theoretical change in the storage modulus $G'$ according to emulsion theories for soft matter. This effect has not been covered in the literature so far. For quantitative description, the well-known Palierne model is used, which can be applied to polymer blends above $T_g$ [12, 13].

The Palierne model describes the rheological behavior of blends of viscoelastic dispersed phase in a viscoelastic matrix under the assumption of a spherical shape of the dispersed phase and includes the effects of hydrodynamic interaction, the size of the dispersed phase, the size distribution, and the interfacial tension. For low interfacial tension (<1 mN m$^{-1}$) and greater radius of the dispersed phase (>0.1 mm) the Palierne model can be expressed as [14, 15]:

$$G^* = G^*_{ma} \cdot \left(1 + 3\varphi \frac{V_r - 1}{2V_r + 3}\right) \cdot \left(1 + 2\varphi \frac{V_r - 1}{2V_r + 3}\right)^{-1}, \tag{1}$$

where $G^*_{ma}$ is the complex modulus of the pure rubber matrix. $V_r$ is the ratio of the complex modulus of the dispersed GR particles ($G^*_{GR}$) to the complex modulus of the rubber matrix ($G^*_{ma}$) and $\varphi$ is the volume fraction of GR particles.

Both the diffusion of sulfur and the emulsion-like blend of GR particles in the rubber matrix lead to a significant change in $G'$. Therefore, it is challenging to study both effects individually. The simultaneous measurement of molecular and macroscopic properties during vulcanization by the unique Rheo-NMR combination helps to differentiate between these two effects.

### 1.3 | Measurement of the Vulcanization Reaction and CLD

Macroscopically, the rubber vulcanization reaction is typically studied through its time dependent rheological response, such as tracking the development of the storage modulus $G'$ during the formation of a chemically crosslinked network. For this purpose, closed-cavity rheometers (CCR) are commonly utilized in rubber research and industry. The cavity of this instrument is sealed to allow the application of pressure during vulcanization. A grooved cone–cone geometry is used to prevent wall slippage at high strain amplitudes [16]. According to the theory of rubber elasticity, the plateau modulus $G_N$ is proportional to the effective CLD $\nu$ (in mol mm$^{-3}$) of the network at a given temperature $T$ [17], which can be written as:

$$G_N = \nu RT, \tag{2}$$

where $R$ is the universal gas constant. Typically, $G'(t_{vulc})$ [18, 19], the absolute value of the torque $|S^*|(t_{vulc})|$ [5, 9, 20], or the in-phase torque $S'(t_{vulc})$ [3, 11] (reflecting the elastic contribution) are used to monitor the time dependent vulcanization.

On a molecular length scale (<10 nm) [21] the influence of the crosslinking upon the network chain dynamics can be studied by time-domain nuclear magnetic resonance (TD-NMR) utilizing a low-field NMR relaxometer (Larmor frequency range of 10 to 60 MHz). By using pulse sequences such as Hahn echo or Carr–Purcell–Meiboom–Gill (CPMG) it is possible to measure and quantify proton transverse relaxation times, which are sensitive to the local molecular mobility of



10974628, 0, Downloaded from https://onlinelibrary.wiley.com/doi/10.1002/app.71322 by Karlsruher Institut Fur Technologie, Wiley Online Library on [28/08/2026]. See the Terms and Conditions (https://onlinelibrary.wiley.com/terms-and-conditions) on Wiley Online Library for rules of use; OA articles are governed by the applicable Creative Commons License

the polymer segments. An increase in the degree of crosslinking typically results in shorter $^1$H transverse relaxation times ($T_2$) [19, 22–25]. Continuously measuring the average $T_2$ and $T_2$ distributions of the polymer protons by TD-NMR with a time resolution of approximately 30 s is a method monitoring the network constitution. At measurement temperatures well above the glass transition $T_g$ (typically $T > T_g + 100$ K), the NMR transverse relaxation ($T_2$–) of rubber is dominated by the fluctuating motion between crosslinks and is therefore a function of the CLD. Additionally, at these temperatures $T_2$ is rather independent of the temperature [24–28].

For crosslinked polymers, extensive studies have been conducted to establish a molecular-macroscopic correlation by measuring both the macroscopic modulus through rheological methods and the microscopic dynamics via TD-NMR measurements [18, 19, 22, 24, 29–31]. These studies indicate that at the above mentioned temperatures, the inverse transverse relaxation time ($T_2^{*-1}$) increases linearly with the molecular weight of the network chains (typical slope of 1 kg mmol$^{-1}$ s$^{-1}$ [22]).

The group of Wilhelm developed a setup that couples a high-end plate–plate rheometer with a low-field NMR relaxometer (abbreviated "Rheo-NMR") and thus provides the opportunity to obtain an in situ molecular-macroscopic correlation of various polymer materials [19, 21, 32–34]. This unique setup correlates both parameters, $G'$ and $T_2^{*-1}$. That addresses the frequently encountered issues related to correlation measurements obtained from different devices, as varying methods may differ in sample preparation, experimental design, and measurement conditions, such as heating rate, exact temperature, or thermal conductivity. Consequently, direct correlation of such data is rare. Nie et al. applied Rheo-NMR to compare conventional and efficient vulcanization systems and obtained a direct molecular-macroscopic correlation between $G'$ and $T_2^{*-1}$ [19].

### 1.4 | Scope of This Article

This article presents an analysis of vulcanization in pure and GR loaded rubber compounds by Rheo-NMR. During the vulcanization of six different rubber compounds, both the rheological characterization and the TD-NMR experiments were carried out simultaneously. Each data set was analyzed to evaluate the vulcanization reaction measured with the different methods to assess the impact of the GR loading. Additionally, the direct $G'$-$T_2^{*-1}$-correlation was analyzed for the pure compounds during vulcanization. The Palierne model was used to compare the results with theoretical predictions with the measured data of $G'$. In addition, the resulting change in the transverse relaxation time of the GR particles $T_2^{*-1}$ is determined and analyzed to assess the further vulcanization of the GR particles.

## 2 | Materials and Methods

The studied materials are identical to those used by Frosch et al. [35]. The sample processing is the same as the processing in the cited article.

### 2.1 | Rubber Compound Formulations and Mixing Conditions

In the presented study two different basic rubber formulations based on natural rubber (NR) and styrene-butadiene rubber (SBR) were investigated. The different formulations with their respective amount of GR, including the trade names of each component, are shown in ref. [35].

The GR is produced the same way as the pure compounds, but is vulcanized, cryogenic ground, and then mixed into the respective matrix compound.

Throughout this article the pure rubber compounds without GR are named NR$_{ma}$ and SBR$_{ma}$ rubber compounds and serve as reference samples. The SBR$_{ma}$ compounds and the GR loaded rubber compounds with SBR in the rubber matrix will be called SBR compounds and vice versa. In diagrams a SBR rubber compound is shown with a violet rectangle and NR compounds are shown with a turquoise rectangle. Additionally, GR loading is indicated with circles inside this rectangle with their associated color.

Table 1 shows a comparison of some selected molecular properties of the two polymers used.

The detailed procedure for mixing the different samples is described by Frosch et al. [35]. In this article, six samples with the respective volume fraction of GR particles were analyzed as shown in Table 2. The volumetric fraction of the GR particle in the rubber compounds is in all combinations very similar and corresponds to an typical used level, while higher concentrations (< 50%) are with certain adjustments reachable [38].

### 2.2 | Vulcanization Kinetics Using a Closed-Cavity Rheometer

A SIS V50 from TA Instruments, Eschborn, Germany (former Scarabaeus) was used to analyze the vulcanization kinetics

**TABLE 1** | Comparison of the molecular properties of the used polymers for the different compounds and GR particles.

| Polymer | Density [kg l$^{-1}$] | Trans-1,4-content [%] | Cis-1,4-content [%] | Vinyl-1,2-content [%] | $T_g$ [°C] | Mooney viscosity[c] [MU] |
|---|---|---|---|---|---|---|
| NR | 0.93[b] | < 1[b] | 99[b] | < 1[b] | −73[b] | 50.7 |
| SBR | 0.94[a] | 76[a] | 9[a] | 15[a] | −50[b] | 49[a] |

[a]Taken from ref. [36].
[b]Taken from ref. [37].
[c]ML (100°C, 1 + 4 min).



10974628, 0, Downloaded from https://onlinelibrary.wiley.com/doi/10.1002/app.71322 by Karlsruher Institut Fur Technologie, Wiley Online Library on [28/08/2026]. See the Terms and Conditions (https://onlinelibrary.wiley.com/terms-and-conditions) on Wiley Online Library for rules of use; OA articles are governed by the applicable Creative Commons License

**TABLE 2** | Studied samples in this article with their respective calculated compound density $\rho$ and the volume fraction $\varphi$ of the GR particles in the rubber compound.

| Sample notation | Symbol in diagrams | Matrix polymer | GR polymer | $\rho\left[\text{kg l}^{-1}\right]$ | $\varphi$ (GR particles) [%] |
|---|---|---|---|---|---|
| $NR_{ma}$ | | NR | — | 1.131 | — |
| $NR_{ma} + NR_{GR}$ | | NR | NR | 1.131 | 15.8 |
| $NR_{ma} + SBR_{GR}$ | | NR | SBR | 1.132 | 15.6 |
| $SBR_{ma}$ | | SBR | — | 1.140 | — |
| $SBR_{ma} + SBR_{GR}$ | | SBR | SBR | 1.140 | 15.8 |
| $SBR_{ma} + NR_{GR}$ | | SBR | NR | 1.139 | 15.9 |

*Note:* Sample notation follows the following principle: >matrix polymer<$_{ma}$ +>Ground rubber polymer<$_{GR}$.

of all samples as a reference. A time sweep was conducted at $T = 160^{\circ}$C, with an angular frequency of $\omega / 2\pi = 1.67$ Hz, and an oscillation strain amplitude of $\gamma_0 = 0.5\,\%$.

## 2.3 | Rheo-NMR

### 2.3.1 | Rheo-NMR Setup

There are different hyphenated Rheo-NMR setups with their respective applications. A combination of high-field NMR with a simple shear experiment is used to evaluate shear fields [39–44]. With a unique combination of a compact low-field NMR magnet and a high-end oscillatory rheometer we can carry out rheological characterization in shear, both in the linear and nonlinear regime. The detailed device descriptions are named at the end of this section. The latter setup is used in this article. A schematic overview of this setup and the magnet has been published multiple times [19, 21, 32–34]. The magnet is constructed with NdFeB magnet bars in a Halbach array to create a static homogeneous magnetic field ($\Delta B_0 / B_0 \approx 1 \cdot 10^{-3}$) with a field strength of $\Delta B_0 \approx 0.59$ T, which corresponds to a 1H Larmor frequency of $\omega_L / 2\pi \approx 25$ MHz. The pulse lengths for 90° and 180° are $t_{90} = 2.8\ \mu s$ and $t_{180} = 5.4\ \mu s$, respectively [32]. The receiver dead time was determined to be 10 μs. During the Rheo-NMR measurement, the magnet was electrically heated and kept constant at 45°C to reduce the drift of the $B_0$ field. The rheological measurements were conducted using a ceramic plate–plate geometry with 13 mm. The design of the probe, the heating unit, the thermal isolation, and the magnetic-field shielding can be found in ref. [32]. A DHR 3 (TA Instruments, USA) was used for rheological measurements. During vulcanization, the temperature of the sample was controlled by a Bruker Variable Temperature (BVT) unit (Bruker, Rheinstetten, Germany). A nitrogen gas flow of 900 L min$^{-1}$ was used to heat and to prevent sample oxidation.

TD-NMR data were measured using a Minispec mq20 amplifier from Bruker, Rheinstetten, Germany. The rheological data were measured using a DHR-3 from TA Instruments, Eschborn, Germany.

## 2.4 | Measurement of Rheology and TD-NMR by Rheo-NMR

The rubber compounds were pressed into 1.5 mm sheets at 40°C for 3 min, to avoid crosslinking and then disks with a diameter of 10 mm were punched. The samples were then loaded in a few seconds onto the upper plate and then the geometry was closed at a normal force of 0.3 N (resulting in an initial pressure of 96 Pa). After $t_{vulc} > 100$ s the normal force was increased to 40 N (resulting in a final pressure of 32 kPa) to prevent the formation of bubbles inside the rubber compound due to vulcanization. This time was found to be as late as possible to prevent significant flow of the rubber from getting out of the geometry, but as early as needed to prevent the formation of bubbles. The procedure results in a sample with 13 mm and no bubbles after vulcanization.

All isothermal crosslinking experiments were carried out at $T_{vulc} = 140^{\circ}$C, 150°C, and 160°C. Two vulcanization experiments were performed for each rubber compound to assess the reproducibility. The time dependent rheological properties were quantified by dynamic time sweep at $\omega / 2\pi = 1.67$ Hz and at a strain amplitude of $\gamma_0 = 1\,\%$ using a grooved plate–plate geometry to prevent wall slippage.

Simultaneous TD-NMR transverse relaxation measurements were continuously executed with a combined pulse sequence of a magic sandwich echo (MSE) and multiple echoes of "xx4." The xx4 is a CPMG (based on Carr and Purcell [45] and Meiboom and Gill [46]) pulse sequence with 180° phase shifting after each 180°-pulse, which can prevent spin-locking [47]. Several authors report that the $T_2$ determined by a CPMG pulse sequence depends on the pulse spacing [48, 49]. To avoid any confusion about the determined value of $T_2$, it will be named as an apparent transverse relaxation time, $T_2^{*-1}$, which still reflects the semi-local molecular dynamics. The recycle delay (RD) was set as 2.5 s, corresponding to five times the longitudinal relaxation time $T_1$, to provide quantitative relaxation of the protons. During vulcanization the decaying transverse magnetization intensity $I\left(t_{vulc}\right)$ from the MSE-xx4 pulse sequence was recorded as a function of the total sequence time $\Delta\tau_{xx4}$, with eight scans applied for each NMR relaxation signal. This results in a $t_{NMR} = 29.5$ s for each TD-NMR data point



10974628, 0, Downloaded from https://onlinelibrary.wiley.com/doi/10.1002/app.71322 by Karlsruher Institut Fur Technologie, Wiley Online Library on [28/08/2026]. See the Terms and Conditions (https://onlinelibrary.wiley.com/terms-and-conditions) on Wiley Online Library for rules of use; OA articles are governed by the applicable Creative Commons License

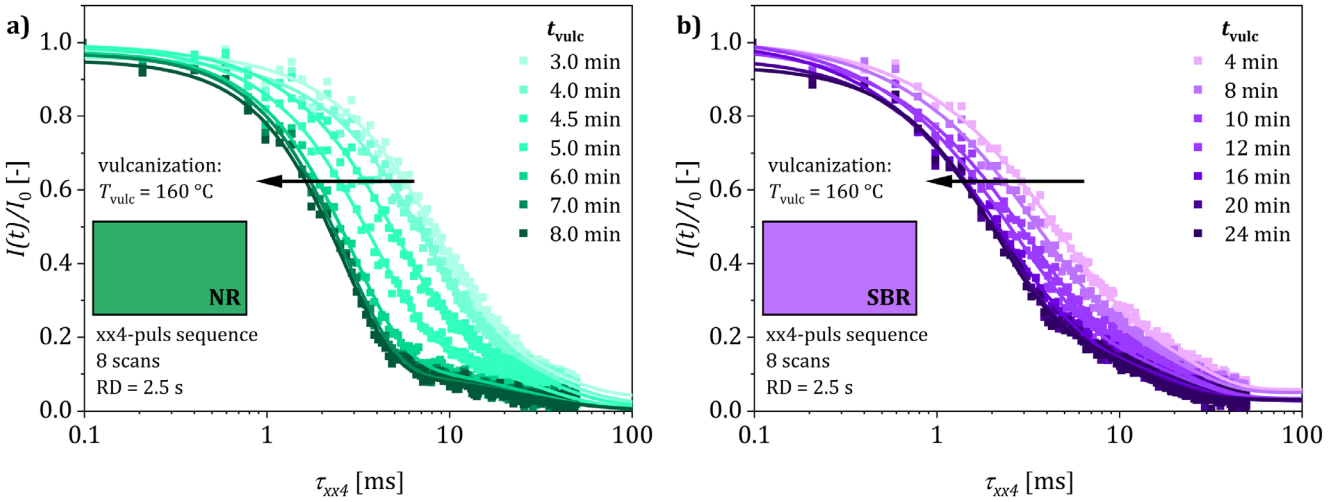


**FIGURE 2** | An example of the evolution of normalized magnetization $I(\tau)/I_0$ during vulcanization from TD-NMR measurements with the xx4-CPMG pulse sequence at specially selected $t_{vulc}$. $I_0$ is defined as the first measured $I(\tau = 0.01\,\mu s)$. In (a) the evolution of the signal of the $NR_{ma}$ compound and in (b) of the $SBR_{ma}$ compound can be seen. The data were fitted using Equation (4). The resulting $T_2^{*-1}$ can be found in Figure 5 at all measured $t_{vulc}$. The MSE signal was not used for investigation, consequently not shown. [Color figure can be viewed at wileyonlinelibrary.com]

$T_2^{*-1}$, extracted from fitting the relaxation curve obtained (see below). The xx-4 pulse sequence was applied with a spacing time $2\Delta\tau_{xx4} = 200\ \mu s$ and 512 echoes.

### 2.4.1 | TD-NMR Data Analysis

The TD-NMR data were analyzed using the transverse relaxation time $T_2$. The $T_2$ is more strongly influenced by the strength of local proton–proton spin–spin interactions (< 2 nm) in a rubber network at temperatures much higher than $T_g$. Therefore, $T_2$ is sensitive to the density and motion constraints of the chemical and physical network junctions in rubber. At temperatures far above $T_g$ ($T > T_g + 100$ K), segmental motion of the polymer in crosslinked rubber networks (typical correlation time of fast local segmental motion $\tau_{fast} < 10^8\ s$) is inherently anisotropic. The reason is either a restriction by the permanent chemical crosslinks or a limitation of the reptation tube confined by temporary and trapped chain entanglements [50–53]. A small fraction $q$ ($q \approx 10^{-4}$) of the dipolar interaction is retained at a slow correlation time $\tau_{slow}$ (typically $\tau_{slow} = 10^{-3}$ s) of the overall motion of the entire network chain. The relaxation of the magnetization of the free chain ends is estimated to decay purely exponentially. This assumption leads to the following fit equation for the total magnetization decay according to published literature [24, 28, 29, 53]:

$$I(\tau) = I_{ma}\exp\left\{-\frac{\tau}{T_2} - qM_2\tau_{slow}^2\left[\exp\left(-\frac{\tau}{\tau_{slow}}\right) + \frac{\tau}{\tau_{slow}} - 1\right]\right\} + I_{ce}\exp\left(-\frac{\tau}{T_2}\right), \tag{3}$$

where $I(\tau)$ is the magnetization intensity, $T_2$ is the characteristic transverse relaxation time, and $I_{ma}$ and $I_{ce}$ are the fractions of the network chains and free dangling chain ends, respectively. A Weibull-type exponential decay function can be used to simplify the anisotropic movement [19, 54, 55]. Then, the decay of magnetization can be expressed in a simplified way:

$$I(\tau) = I_{ma}\exp\left[-\left(\frac{\tau}{T_{2,ma}^*}\right)^{\beta}\right] + I_{ce}\exp\left(-\frac{\tau}{T_{2,ce}^*}\right) + y_0, \tag{4}$$

with a factor $\beta = 0.5 - 2$. The introduced subscripts "ma" and "ce" indicate the fast magnetization decay of the matrix polymer motion and the slow, chain end magnetization decay, reflecting the mobile polymer motion, respectively. The fractions $I_{ma}$ and $I_{ce}$ are the corresponding fractions of protons, which describe the fast and the slow relaxation, respectively.

Figure 2 shows the time evolution of the normalized magnetization during the CPMG pulse sequence during the vulcanization of (a) the $NR_{ma}$ compound and (b) the $SBR_{ma}$ compound. The relaxation behavior of the rubber magnetization was described by Equation (4). The parameter $\beta$ was determined to be around 1.4 and 1.0 for the investigated NR and SBR compounds, respectively, while $T_{2,ce}^{*-1}$ was kept unchangeable for all fits to be 25 ms for all samples. These determined $\beta$ and $T_{2,ce}^{*-1}$ parameters were fixed for the further fitting procedure to reduce the total number of free fit parameters.

The GR loaded compounds show a combined signal of the GR particles and the rubber matrix. Due to this a second, fast relaxing term is used (subscript "GR") to describe the magnetization decay of the GR particles. The resulting equation can be found in Equation (5).

$$I(\tau) = I_{ma}\exp\left[-\left(\frac{\tau}{T_{2,ma}^*}\right)^{\beta_{ma}}\right] + I_{GR}\exp\left[-\left(\frac{\tau}{T_{2,GR}^*}\right)^{\beta_{GR}}\right] + I_{cc}\exp\left(-\frac{\tau}{T_{2,cc}^*}\right) + y_0, \tag{5}$$

with the factors $\beta_{ma}$ and $\beta_{ma} = 0.5 - 2$.

However, observations indicate that distinguishing between the signals of the GR particles and the surrounding rubber matrix



10974628, 0, Downloaded from https://onlinelibrary.wiley.com/doi/10.1002/app.71322 by Karlsruher Institut Fur Technologie, Wiley Online Library on [28/08/2026]. See the Terms and Conditions (https://onlinelibrary.wiley.com/terms-and-conditions) on Wiley Online Library for rules of use; OA articles are governed by the applicable Creative Commons License

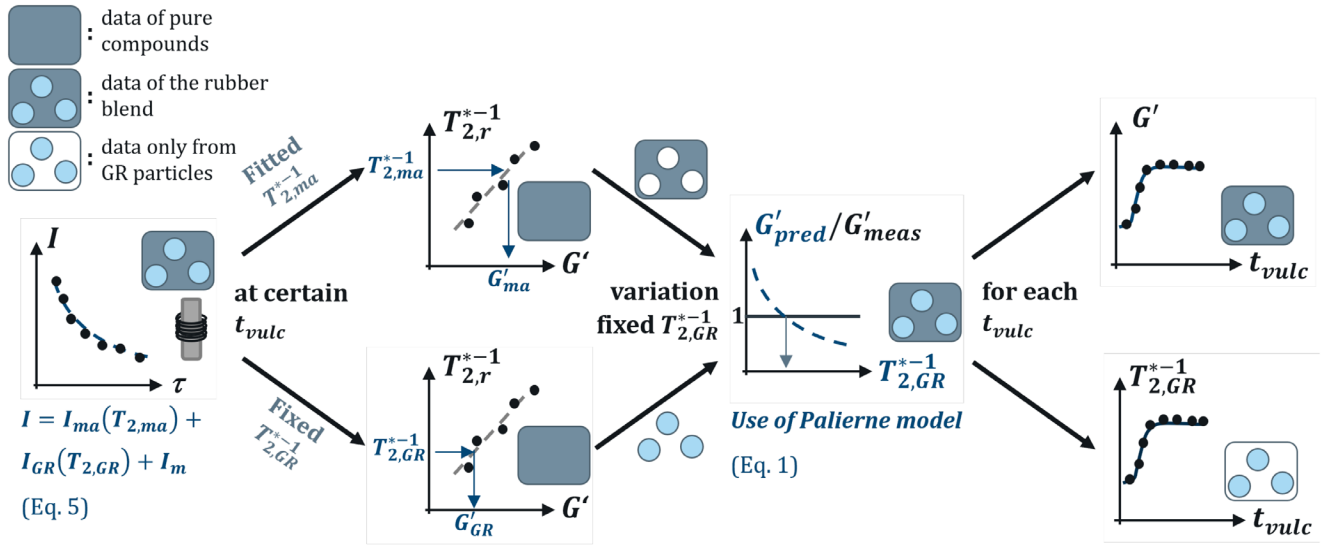


**FIGURE 3** | Procedure used to calculate the $G'$ prediction for the GR loaded compounds using the results from the Rheo-NMR of the pure compounds. $T^{*-1}_{2,GR}$ and $T^{*-1}_{2,ma}$ are used to determine the respective $G'$. The Palierne model is calculated using the different resulting $G^*$. To calculate $G^*$, $G''$ is interpolated using $G'$ of the pure compounds. [Color figure can be viewed at wileyonlinelibrary.com]

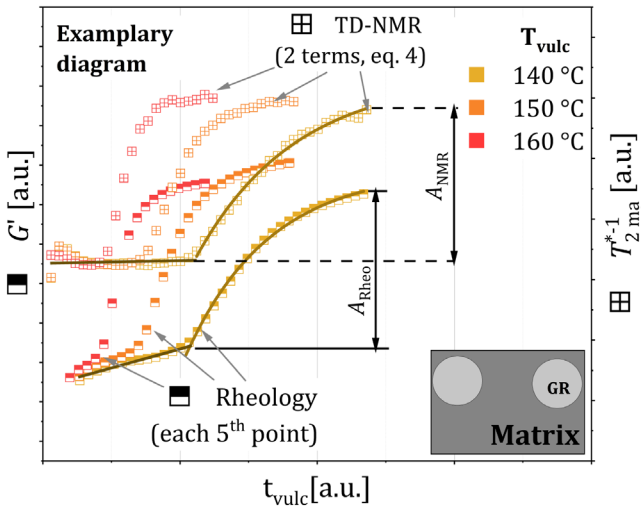


**FIGURE 4** | Exemplary diagram for the vulcanization measured using the Rheo-NMR, showing how to read the diagram. The different colors indicate the respective vulcanization temperature. The different filling indicates by measurement method. The schematic picture at bottom right shows, the respective compound. Pure compounds are shown without circles, GR loaded compounds shown with circles. The amplitudes of vulcanization $A_{Rheo}$ and $A_{NMR}$ were determined by using the difference between the last point and the point at the end of incubation time. Incubation time was determined as the crossover of the linear fit at the first part and the monoexponential fit in the second part. [Color figure can be viewed at wileyonlinelibrary.com]

remains challenging only using TD-NMR. This differentiation can be realized by combining the TD-NMR data to the rheology data using an constitutive model and then comparing this with the measured rheological results. The procedure for achieving this is described below. $T^{*-1}_{2,ce}$ was kept fixed at 0.04 ms$^{-1}$ for all fitting procedures.

#### 2.4.2 | Calculation Procedure for $G'$ Using the Palierne Model

The Palierne model uses the $G^*$ of both the rubber matrix and of the GR particles, $G^*_{ma}$ and $G^*_{GR}$, respectively, to calculate $G^*$ of the blend. To extract $G'$ from the Rheo-NMR data a four steps procedure needs to be applied. The graphical overview of this procedure is shown in Figure 3.

The first step is to determine $T^{*-1}_{2,ma}$ by fitting Equation (5) to the TD-NMR data, while keeping $T^{*-1}_{2,GR}$ fixed at a certain value. In the second step, these two values are then used to interpolate to $G'_{ma}$ and $G'_{GR}$, respectively, by using the $T^{*-1}_2$ vs. $G'$-correlation of the pure compounds. In the third step, $G'_{ma}$ and $G'_{GR}$ are used to interpolate for the respective $G''$. These values are used to calculate the $G'$ of the blend by applying the Palierne model (Equation 1). In the last step, this procedure is repeated iteratively until the highest agreement of the predication by the Palierne model and measured $G'$ is received ($G'_{pred}/G'_{meas} \approx 1$). A direct fit of both parameters is not applicable, because the fit procedure is not robust enough. Therefore, this procedure helps to validate the fit results of the individual $T^{*-1}_{2,ma}$ and $T^{*-1}_{2,GR}$ by applying their rheological prediction to the measured. Without the simultaneous measurement of Rheology and TD-NMR this would not be possible.

## 3 | Results and Discussion

### 3.1 | Vulcanization Kinetics

The vulcanization related properties ($T^{*-1}_{2,ma}(t_{vulc})$ and $G'(t_{vulc})$) can be measured simultaneously by the unique hyphenated Rheo-NMR setup. Figure 4 shows an example of such a measurement at three different $T_{vulc}$. A detailed explanation can be found in the caption of that figure.



10974628, 0, Downloaded from https://onlinelibrary.wiley.com/doi/10.1002/app.71322 by Karlsruher Institut Fur Technologie, Wiley Online Library on [28/08/2026]. See the Terms and Conditions (https://onlinelibrary.wiley.com/terms-and-conditions) on Wiley Online Library for rules of use; OA articles are governed by the applicable Creative Commons License

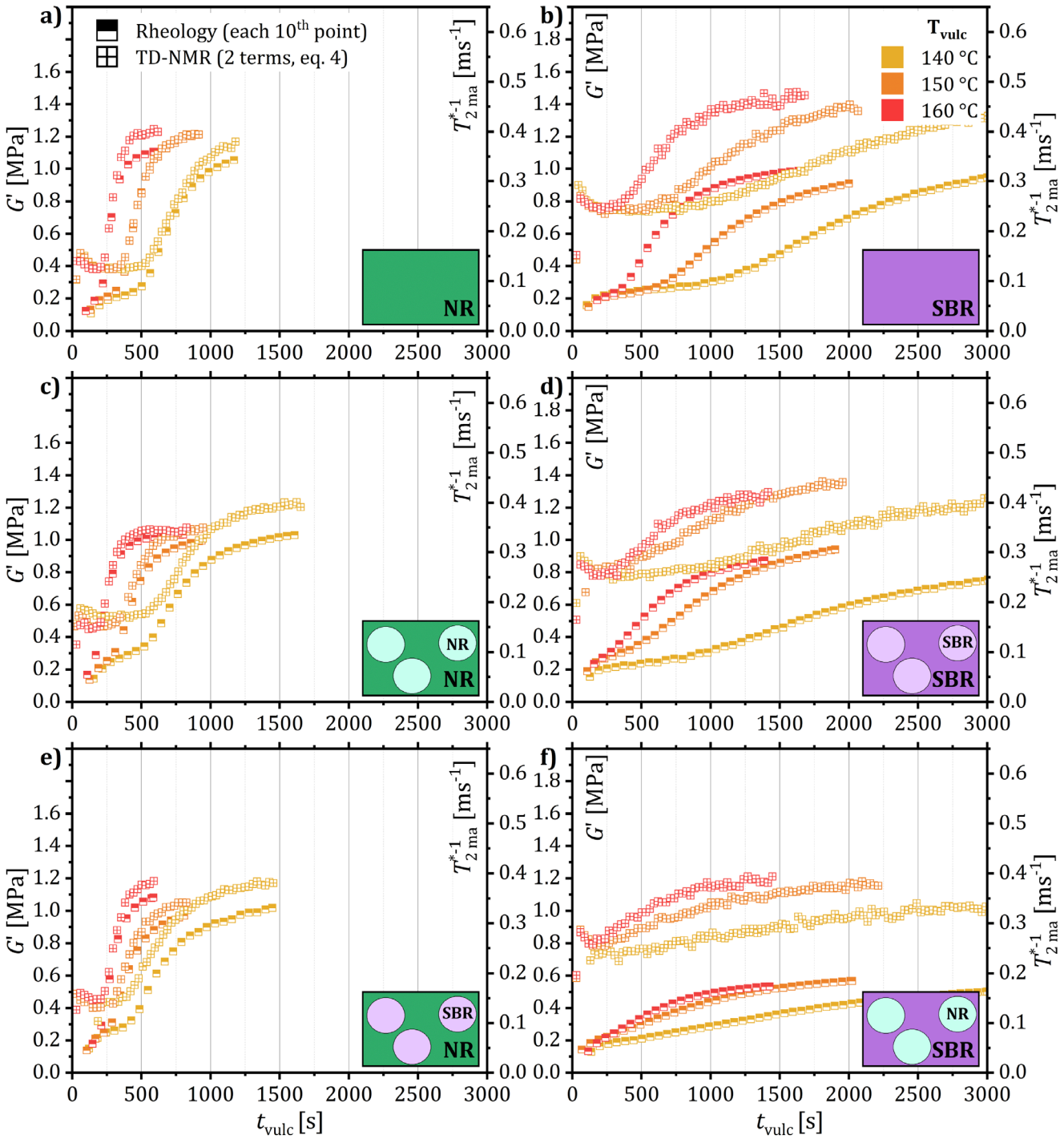


**FIGURE 5** | The $G'$ (▬) and $T_{2,ma}^{*-1}$ (⊞) from the simultaneously measured rheology and TD-NMR during vulcanization of the pure and GR loaded (30 phr) rubber compounds at various vulcanization temperatures. The graphs show the vulcanization of the pure rubber compounds in (a) and (b), the rubber compounds with GR particles based on the same polymer as the rubber matrix in (c) and (d), and the rubber compounds with GR particles based on the contrary polymer in (e) and (f). The various Amplitudes $A$ due to vulcanization are used in Table 3 exemplary shown in (a) and (c) to quantify the impact of GR loading on the final CLD. [Color figure can be viewed at wileyonlinelibrary.com]

The results of these measurements are shown in Figure 5 for both materials of the pure rubber matrix in (a, b) and the GR loaded rubber compounds studied in (c–f).

The vulcanization can be quantified using the resulting amplitudes $A_{Rheo}$ and $A_{NMR}$ as shown in Figure 5 for the rheology and TD-NMR data, respectively. These amplitudes are used to analyze the impact of GR loading on the CLD, since the amplitude $A$ correlates with CLD. For better comparison, the amplitude of the GR loaded compound ($A_{GR}$) is normalized to the amplitude of the pure compound ($A_{pure}$) of the respective matrix polymer. The amplitude is also determined during vulcanization using the CCR. All results are shown in Table 3.



10974628, 0, Downloaded from https://onlinelibrary.wiley.com/doi/10.1002/app.71322 by Karlsruher Institut Fur Technologie, Wiley Online Library on [28/08/2026]. See the Terms and Conditions (https://onlinelibrary.wiley.com/terms-and-conditions) on Wiley Online Library for rules of use; OA articles are governed by the applicable Creative Commons License

The rheological data determined by Rheo-NMR and by the CCR at all measured $T_{vulc}$ exhibit agreement in the range of the standard deviation for all samples, validating the Rheo-NMR measurements. All GR loaded compounds exhibit a decrease in the amplitude compared to the pure rubber matrix compound (indicated by a value $<1$). This decrease measured with rheology (Rheology in Rheo-NMR and CCR) and TD-NMR show the same level for most samples. In contrast, the $SBR_{ma} + NR_{GR}$ shows higher deviation between rheology (51% decrease) and TD-NMR (32% decrease). It should also be pointed out that the effect is similar at all $T_{vulc}$ indicated by the low standard deviation.

The explanation for this difference may lie in the different effects detected by rheology and TD-NMR (Figure 1). Although rheology is influenced by both a decrease in the final CLD as a result of sulfur diffusion and a change due to the emulsion-like blending of the GR particles in the rubber matrix, TD-NMR only measures the decrease in the final CLD. We can assume that $A_{GR}$ of rheology and TD-NMR show the same reduction due to the reduced CLD resulting from sulfur diffusion, if the type of crosslinks arising remain the same as in the pure compounds [19]. Therefore, there is an additional reduction of up to 29%, which is not only explained by sulfur diffusion. The agreement between the rheology obtained from Rheo-NMR and CCR indicates that the two methods can be reliably compared.

Such a shown reduction in CLD, represented by $A_{GR}/A_{pure}$, typically leads to lower hardness, tensile strength, and elasticity [3], emphasizing the practical importance of this effect. The Palierne model is used to assess the effect of the emulsion-like blend of GR particles in the rubber matrix on the rheological properties.

**TABLE 3** | The ratio of the respective determined amplitude during vulcanization of the GR loaded compound ($A_{GR}$) to the amplitude of the pure compound ($A_{pure}$) at all $T_{vulc}$.

| | $A_{GR}/A_{pure}$ [−] | | | | | |
|---|---|---|---|---|---|---|
| **Rubber compound** | **via rheology (by CCR)** | | **via rheology (by Rheo-NMR)** | | **via TD-NMR (by Rheo-NMR)** | |
| $NR_{ma} + NR_{GR}$ | 0.80 | ±0.04 | 0.73 | ±0.06 | 0.83 | ±0.07 |
| $NR_{ma} + SBR_{GR}$ | 0.87 | ±0.04 | 0.93 | ±0.04 | 0.95 | ±0.10 |
| $SBR_{ma} + SBR_{GR}$ | 0.83 | ±0.03 | 0.86 | ±0.08 | 0.88 | ±0.03 |
| $SBR_{ma} + NR_{GR}$ | 0.50 | ±0.03 | 0.49 | ±0.03 | 0.68 | ±0.04 |

*Note:* This indicates the drop of the respective property due to the GR loading. Two samples were measured at each $T_{vulc}$. Therefore, the values shown represent the mean and standard deviation calculated from six measurements.

## 3.2 | Molecular-Macroscopic Correlation by Rheo-NMR

The simultaneous measurement of rheology data and TD-NMR data enables a direct correlation of macroscopic-molecular properties. To obtain this correlation, $G'(t_{vulc})$ is interpolated to match the corresponding $t_{vulc}$ measured by TD-NMR. Figure 6 shows the results for the pure rubber compounds studied.

To assess the influence of the GR particles on the rheological properties, the theoretical prediction of $G^*$ is calculated using these molecular-macroscopic correlations and the Palierne model according to Figure 3. The comparison of the prediction and the measured data is depicted in Figure 7.

The prediction made by the Palierne model describes the data of all compounds with a deviation of up to 5%. Only the compounds $NR_{ma} + NR_{GR}$ and $SBR_{ma} + NR_{GR}$ at $T_{vulc} = 140°C$ show higher deviations of up to 15%. This leads to the conclusion that the Palierne model can be used to describe GR loaded compounds with the given uncertainties.

Nevertheless, the difference in the predictability for $NR_{GR}$ compared to $SBR_{GR}$ at $T_{vulc} = 140°C$ shows a still unknown effect. Since this effect is independent of the used matrix and only

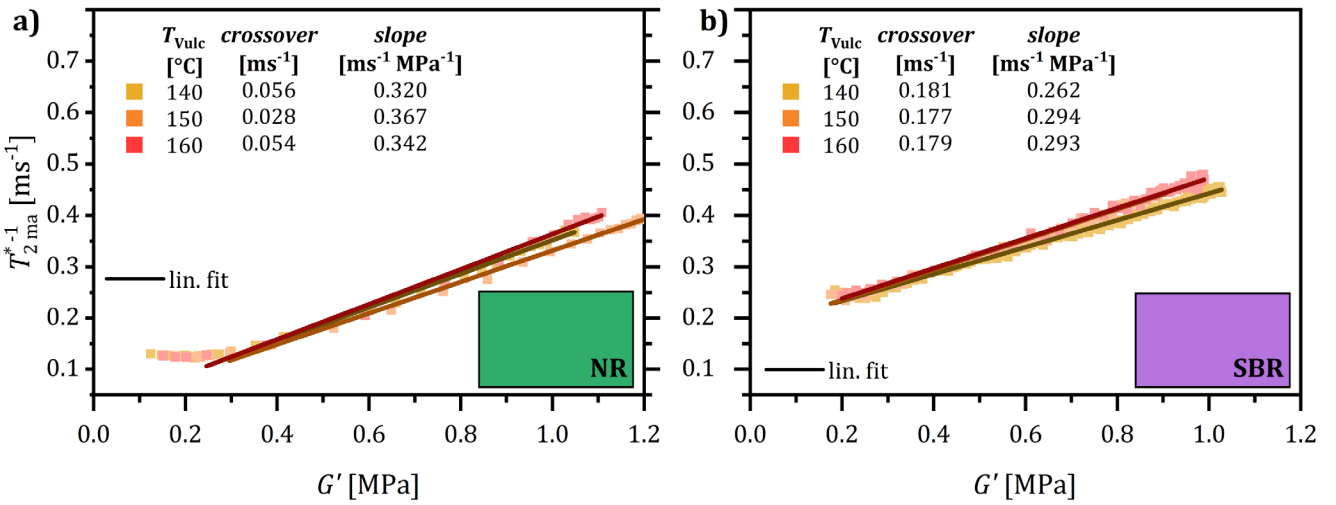


**FIGURE 6** | Direct correlation of the molecular influenced $T^{*-1}_{2,ma}$ versus the macroscopic property $G'$, which indicates the relation of segmental mobility to macroscopic behavior. The correlation is shown for the pure rubber compounds without GR. (a) The $NR_{ma}$ compound and (b) the $SBR_{ma}$ compound. [Color figure can be viewed at wileyonlinelibrary.com]



10974628, 0, Downloaded from https://onlinelibrary.wiley.com/doi/10.1002/app.71322 by Karlsruher Institut Fur Technologie, Wiley Online Library on [28/08/2026]. See the Terms and Conditions (https://onlinelibrary.wiley.com/terms-and-conditions) on Wiley Online Library for rules of use; OA articles are governed by the applicable Creative Commons License

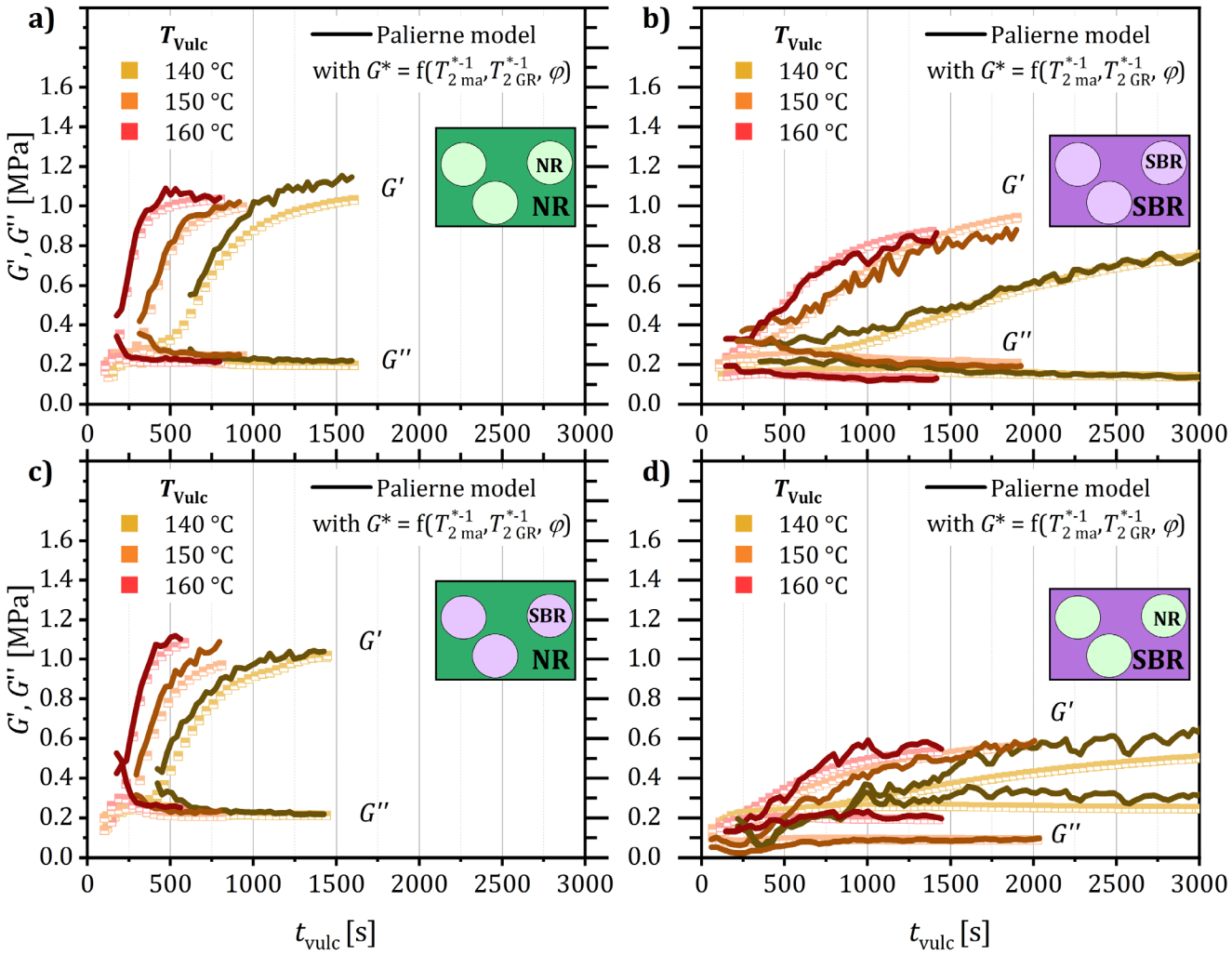


**FIGURE 7** | The measured macroscopic property $G'$ and $G''$ and the respective prediction made using the Palierne model. The results are shown for the rubber compounds with GR particles based on the same polymer as the rubber matrix in (a, b), and the rubber compounds with GR particles based on the contrary polymer in (c, d). [Color figure can be viewed at wileyonlinelibrary.com]

at a certain $T_{vulc}$ a GR related property should be the reason. According to the Palierne model, differences in interfacial interactions should not significantly influence the data at the observed order of magnitude [15]. A difference in the resulting cross-link structure (more polysulfidic crosslinks) at the given conditions for $NR_{GR}$ may explain this deviation by changing the $G'$-$T_2^{*-1}$-correlation. This effect is not captured in the used procedure and is well described by Nie et al. [19].

The applied procedure also gives information about the further vulcanization of the GR. This is shown in Figure 8 for the compounds studied.

The results show that the $NR_{GR}$ behaves differently compared to the $SBR_{GR}$. The $NR_{GR}$ shows an increase in $T_{2,GR}^{*-1}$ during vulcanization indicating a further increase in CLD. The final increase is approximately 87.5% within the NR matrix and approximately 100% within the SBR matrix compared to the final $T_{2,ma}^{*-1}$ of the $NR_{ma}$ compound. The $SBR_{GR}$ does not show a clear change in $T_{2,GR}^{*-1}$ during vulcanization itself, indicating that there is no further vulcanization. Additionally, $T_{2,GR}^{*-1}$ of $SBR_{GR}$ is lower than the final $T_{2,ma}^{*-1}$ of the $SBR_{ma}$ compound by 12.5%.

The hypothesis is that $NR_{GR}$ increases sulfur diffusion from matrix to the GR particles. The explanation might be due to a higher vulcanization rate of NR compared to SBR as can be seen in Figure 5, which increases the chemical potential of free sulfur during the vulcanization and promotes diffusion. Additionally, the NR compound shows a higher coefficient of diffusion according to ref. [56]. This explanation agrees with the results described in the literature [35, 56]. For the $SBR_{GR}$ we assume that the cryogenic grinding process damages the network of $SBR_{GR}$, what reduces the CLD of this network. This can be explained by higher $T_g$ of the used SBR compared to the used NR (see Table 1). The higher $T_g$ broadens the brittle regime of that material and increases therefore the mechanochemical impact of the cryogenic grinding on the polymer network.

## 4 | Conclusion and Outlook

This article investigated the effect of GR loading of rubber compounds. The unique hyphenated Rheo-NMR setup was used to quantify the effect on the rheological behavior as an emulsion-like blend as well as on the further vulcanization of the GR particle due to sulfur diffusion.



10974628, 0, Downloaded from https://onlinelibrary.wiley.com/doi/10.1002/app.71322 by Karlsruher Institut Fur Technologie, Wiley Online Library on [28/08/2026]. See the Terms and Conditions (https://onlinelibrary.wiley.com/terms-and-conditions) on Wiley Online Library for rules of use; OA articles are governed by the applicable Creative Commons License

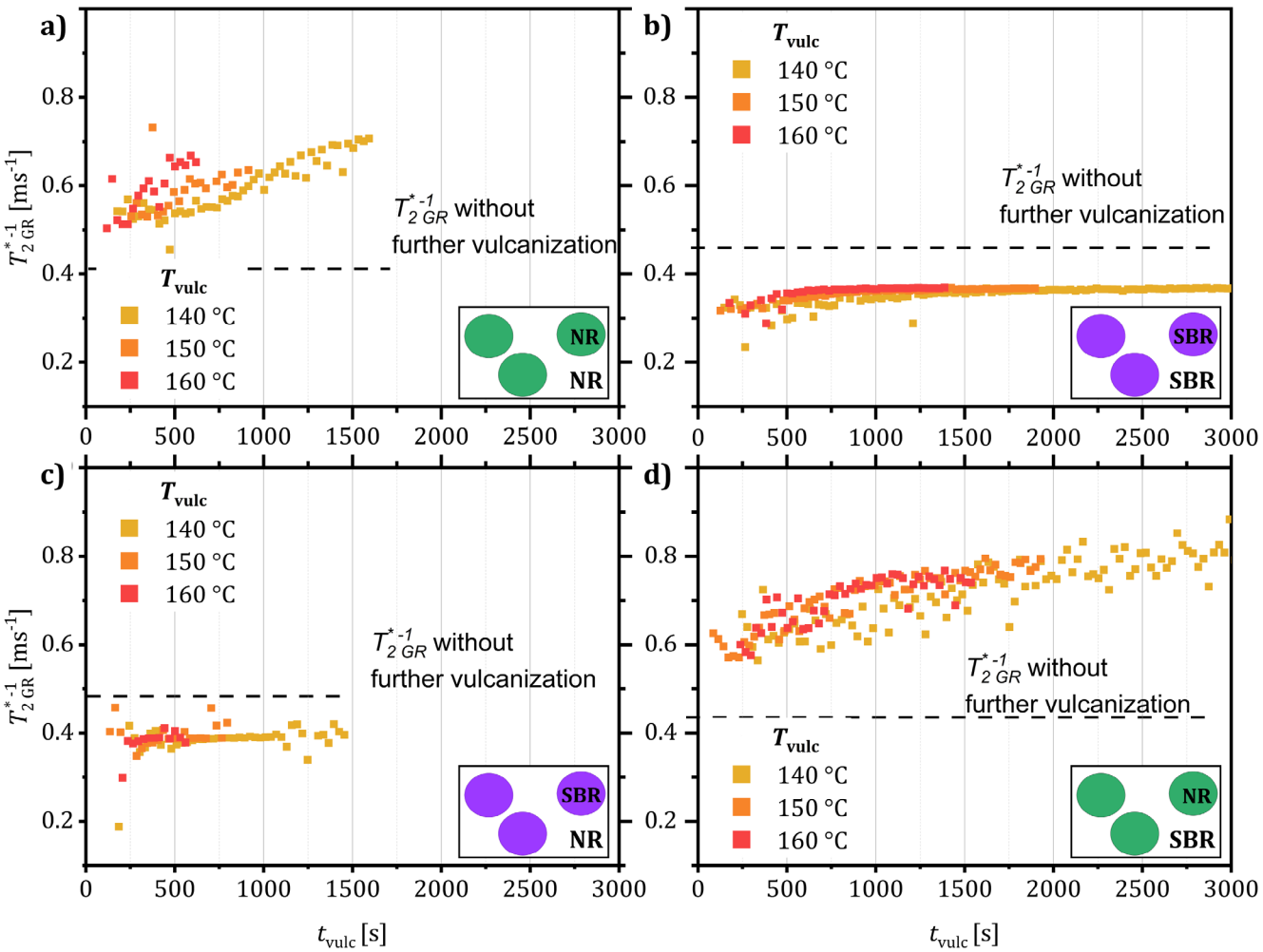


**FIGURE 8** | Resulting $T^{*-1}_{2,GR}$ of the GR particles achieved by comparing the prediction made with the Palierne model with the measured data. The results are shown for the rubber compounds with GR particles based on the same polymer as the rubber matrix in (a, b), and the rubber compounds with GR particles based on the contrary polymer in (c, d). $NR_{GR}$ shows increase in $T^{*-1}_{2,GR}$ indicating a further vulcanization reaction, while $SBR_{GR}$ shows no change during vulcanization. [Color figure can be viewed at wileyonlinelibrary.com]

GR loading was found to lead to a decrease in final parameters, namely $T^{*-1}_{2,ma}$ and $G'$, consistent with previously published literature [5, 9–11]. This effect is explained in the literature by the diffusion of free $S_8$ sulfur from the rubber matrix into the GR particle. The effect of the emulsion-like blend on the rheological properties of GR loaded compounds has not been covered in literature so far.

The simultaneous measurement of both rheological and time-domain NMR (TD-NMR) data by the Rheo-NMR setup allows to differentiate between the effects of the emulsion-like blending and the change in CLD due to sulfur diffusion. The linear correlation between the TD-NMR data and the rheological properties of the pure compounds received by plotting $T^{*-1}_{2,ma}$ versus $G'$ and the Palierne model are used. By vary $T^{*-1}_{2,GR}$, $G'$ can be predicted for the GR loaded compounds. The Palierne model describes the vulcanization of the GR loaded compounds with a deviation of up to 15%. The resulting $T^{*-1}_{2,GR}$ shows an increase during the vulcanization depending on the polymer in the GR. The $NR_{GR}$ shows an increase of up to 100% independent of the matrix compound, while the $SBR_{GR}$ shows no further increase. This increase may be correlated with an increase in CLD.

This received information is essential to understand and improve the performance of GR loaded compounds. This emphasizes the importance of the use of the Rheo-NMR setup for rubber recycling.

This article deserves as a framework for further studies of GR loading in rubber compounds. Further research should explore different rubbers and variations of crosslinking systems, including alternative accelerators. Additionally, the impact of the particle size of the GR used and concentration should be investigated more in detail. It is also important to detect the maximum concentration of GR, where the Palierne model is applicable. A deeper understanding of all of these effects can help to optimize GR loaded compounds. In addition, a hyphenated Rheo-IR setup [57] can be utilized to validate the results presented in this study and obtain a clearer understanding of the results obtained.

## Author Contributions

**Tim Schülein:** writing – original draft, investigation, conceptualization, methodology, validation, visualization, writing – review and editing, software, formal analysis, project administration, data curation,



10974628, 0, Downloaded from https://onlinelibrary.wiley.com/doi/10.1002/app.71322 by Karlsruher Institut Fur Technologie, Wiley Online Library on [28/08/2026]. See the Terms and Conditions (https://onlinelibrary.wiley.com/terms-and-conditions) on Wiley Online Library for rules of use; OA articles are governed by the applicable Creative Commons License

resources. **Stefan A. Frosch:** writing – review and editing, investigation, methodology. **Manfred Wilhelm:** funding acquisition, writing – review and editing, supervision, resources, project administration. **Volker Herrmann:** supervision, resources, writing – review and editing, funding acquisition, validation, project administration. **Johannes Krückel:** funding acquisition, writing – review and editing, supervision, resources, project administration. **Sarah L. Palloks:** writing – review and editing, software, methodology, investigation.


### Acknowledgments

We thank M. Pollard for proofreading. We thank the companies KLK Emmerich GmbH and Lanxess Deutschland GmbH for providing the stearic acid and the CBS accelerator, respectively. Open Access funding enabled and organized by Projekt DEAL.

### Funding

This research was financially supported by the DKG (German Rubber Society).


### Conflicts of Interest

The authors declare no conflicts of interest.

### Data Availability Statement

The data that support the findings of this study are available from the corresponding author upon reasonable request.

### References


1. European Union: European Commission, "A European Strategy for Plastics in a Circular Economy. COM(2018), (28)," Communication from the Commission to the European Parliament, the Council, the European Economic and Social Committee and the Committee of the Regions, 2018.

2. S. Raffoul, R. Garcia, D. Escolano-Margarit, M. Guadagnini, I. Hajirasouliha, and K. Pilakoutas, "Behaviour of Unconfined and FRP-Confined Rubberised Concrete in Axial Compression," *Construction and Building Materials* 147 (2017): 388–397.

3. V. Herrmann and A. Heinrich, "Influence of the Modification of Ground Truck Tyres as an Additive on the Properties of a Truck Tread Compound," *International Polymer Science and Technology* 44, no. 5 (2017): 1–10.

4. J. Karger-Kocsis, L. Mészáros, and T. Bárány, "Ground Tyre Rubber (GTR) in Thermoplastics, Thermosets, and Rubbers," *Journal of Materials Science* 48, no. 1 (2013): 1–38.

5. S. Li, J. Lamminmäki, and K. Hanhi, "Effect of Ground Rubber Powder on Properties of Natural Rubber," *Macromolecular Symposia* 216, no. 1 (2004): 209–216.

6. H. Liang, D. Rodrigue, and J. Brisson, "Characterization of Recycled Styrene Butadiene Rubber Ground Tire Rubber: Combining X-Ray Fluorescence, Differential Scanning Calorimetry, and Dynamical Thermal Analysis for Quality Control," *Journal of Applied Polymer Science* 132, no. 42 (2015): 42692.

7. A. Phadke and S. De, "Use of Cryoground Reclaimed Rubber in Natural Rubber," *Conservation & Recycling* 9, no. 3 (1986): 271–280.

8. S. Han and M. Han, "Fracture Behavior of NR and SBR Vulcanizates Filled With Ground Rubber Having Uniform Particle Size," *Journal of Applied Polymer Science* 85, no. 12 (2002): 2491–2500.

9. D. Gibala and G. R. Hamed, "Cure and Mechanical Behavior of Rubber Compounds Containing Ground Vulcanizates. Part I—Cure Behavior," *Rubber Chemistry and Technology* 67, no. 4 (1994): 636–648.

10. V. Herrmann, S. Frosch, T. Maslowski, and D. Werner, "Einsatz von definiertem Gummimehl aus NR und SBR in unterschiedlichen Matrixwerkstoffen," *Gummi, Fasern, Kunststoffe* 74, no. 1 (2021): 200–207.

11. V. Herrmann, S. Hanning, and M. Kreyenschmidt, "Untersuchungen zur Diffusion des Schwefels in Rezyklat-Kautschukmischungen - Teil 1: Bestimmung des Diffusionskoeffizienten," *Gummi, Fasern, Kunststoffe* 71 (2018): 232–241.

12. K. Reinheimer, M. Grosso, F. Hetzel, J. Kübel, and M. Wilhelm, "Fourier Transform Rheology as an Innovative Morphological Characterization Technique for the Emulsion Volume Average Radius and Its Distribution," *Journal of Colloid and Interface Science* 380, no. 1 (2012): 201–212.

13. K. Reinheimer, M. Grosso, and M. Wilhelm, "Fourier Transform Rheology as a Universal Non-Linear Mechanical Characterization of Droplet Size and Interfacial Tension of Dilute Monodisperse Emulsions," *Journal of Colloid and Interface Science* 360, no. 2 (2011): 818–825.

14. R. Pal, "A New Linear Viscoelastic Model for Emulsions and Suspensions," *Polymer Engineering & Science* 48, no. 7 (2008): 1250–1253.

15. J. F. Palierne, "Linear Rheology of Viscoelastic Emulsions With Interfacial Tension," *Rheologica Acta* 29, no. 3 (1990): 204–214.

16. T. Schülein, C. K. Georgantopoulos, L. Bolk, V. Herrmann, and M. Wilhelm, "Thermo-Mechanical Degradation Kinetics of a High-Density Poly(Ethylene) Using a Closed-Cavity Rheometer," *Journal of Applied Polymer Science* 142 (2025): e56784.

17. D. W. v. Krevelen and K. t. Nijenhuis, *Properties of Polymers: Their Correlation With Chemical Structure: Their Numerical Estimation and Prediction From Additive Group Contributions*, 4th, completely rev. ed ed. (Elsevier, 2009).

18. A. Mujtaba, M. Keller, S. Ilisch, et al., "Mechanical Properties and Cross-Link Density of Styrene–Butadiene Model Composites Containing Fillers With Bimodal Particle Size Distribution," *Macromolecules* 45, no. 16 (2012): 6504–6515.

19. S. Nie, K.-F. Ratzsch, S. L. Grage, et al., "Correlation Between Macroscopic Elasticity and Chain Dynamics of Natural Rubber During Vulcanization as Determined by a Unique Rheo-NMR Combination," *Macromolecules* 54, no. 13 (2021): 6090–6100.

20. K. Boonkerd, C. Deeprasertkul, and K. Boonsomwong, "Effect of Sulfur to Accelerator Ratio on Crosslink Structure, Reversion, and Strength in Natural Rubber," *Rubber Chemistry and Technology* 89, no. 3 (2016): 450–464.

21. C. Fengler, J. Keller, K. Ratzsch, and M. Wilhelm, "In Situ RheoNMR Correlation of Polymer Segmental Mobility With Mechanical Properties During Hydrogel Synthesis," *Advanced Science* 9, no. 4 (2022): 2104231.

22. V. M. Litvinov, W. Barendswaard, and M. Van Duin, "The Density of Chemical Crosslinks and Chain Entanglements in Unfilled EPDM Vulcanizates as Studied With Low Resolution, Solid State 1H NMR," *Rubber Chemistry and Technology* 71, no. 1 (1998): 105–118.

23. V. M. Litvinov, M. E. Ries, T. W. Baughman, A. Henke, and P. P. Matloka, "Chain Entanglements in Polyethylene Melts. Why Is It Studied Again?," *Macromolecules* 46, no. 2 (2013): 541–547.

24. K. Saalwächter, "Microstructure and Molecular Dynamics of Elastomers as Studied by Advanced Low-Resolution Nuclear Magnetic Resonance Methods," *Rubber Chemistry and Technology* 85, no. 3 (2012): 350–386.

25. G. Simon and H. Schneider, "MC-Determination in Elastomers by $^{1}$H-NMR Relaxation and $^{2}$H-NMR Spectroscopy," *Makromolekulare Chemie, Macromolecular Symposia* 52, no. 1 (1991): 233–246.

26. A. Karekar, K. Oßwald, K. Reincke, B. Langer, and K. Saalwächter, "NMR Studies on the Phase-Resolved Evolution of Cross-Link Densities





10974628, 0, Downloaded from https://onlinelibrary.wiley.com/doi/10.1002/app.71322 by Karlsruher Institut Fur Technologie, Wiley Online Library on [28/08/2026]. See the Terms and Conditions (https://onlinelibrary.wiley.com/terms-and-conditions) on Wiley Online Library for rules of use; OA articles are governed by the applicable Creative Commons License

in Thermo-Oxidatively Aged Elastomer Blends," *Macromolecules* 53, no. 24 (2020): 11166–11177.

27. K. Saalwächter, B. Herrero, and M. A. López-Manchado, "Chain Order and Cross-Link Density of Elastomers as Investigated by Proton Multiple-Quantum NMR," *Macromolecules* 38, no. 23 (2005): 9650–9660.

28. G. Simon, B. Götschmann, D. Matzen, and H. Schneider, "1H-NMR-Spin-Spin Relaxation in Cross-Linked SBR With and Without Carbon Black Filling," *Polymer Bulletin* 21, no. 5 (1989): 475–482.

29. W. Gronski, U. Hoffmann, G. Simon, A. Wutzler, and E. Straube, "Structure and Density of Crosslinks in Natural-Rubber Vulcanizates. A Combined Analysis by NMR Spectroscopy, Mechanical Measurements, and Rubber-Elastic Theory," *Rubber Chemistry and Technology* 65, no. 1 (1992): 63–77.

30. F. Shahsavan, M. Beiner, and K. Saalwächter, "Chain Dynamics in Partially Cross-Linked Polyethylene by Combined Rheology and NMR-Based Molecular Rheology," *Journal of Polymer Science* 60, no. 7 (2022): 1266–1276.

31. P. Zhang, F. Zhao, Y. Yuan, X. Shi, and S. Zhao, "Network Evolution Based on General-Purpose Diene Rubbers/Sulfur/TBBS System During Vulcanization (I)," *Polymer* 51, no. 1 (2010): 257–263.

32. K.-F. Ratzsch, C. Friedrich, and M. Wilhelm, "Low-Field Rheo-NMR: A Novel Combination of NMR Relaxometry With High End Shear Rheology," *Journal of Rheology* 61, no. 5 (2017): 905–917.

33. V. Räntzsch, M. Haas, M. B. Özen, et al., "Polymer Crystallinity and Crystallization Kinetics via Benchtop 1H NMR Relaxometry: Revisited Method, Data Analysis, and Experiments on Common Polymers," *Polymer* 145 (2018): 162–173.

34. V. Räntzsch, M. B. Özen, K.-F. Ratzsch, et al., "Polymer Crystallization Studied by Hyphenated Rheology Techniques: Rheo-NMR, Rheo-SAXS, and Rheo-Microscopy," *Macromolecular Materials and Engineering* 304, no. 2 (2019): 1800586.

35. S. Frosch, V. Herrmann, T. Schülein, F. Grunert, and A. Blume, "Sulfur Diffusion Studies Imitating Recycled Ground-Rubber-Containing Compounds," *Polymers* 16, no. 22 (2024): 3112.

36. GmbH, LD, "Buna SE 1502 L - Product Data Sheet" (2010).

37. F. Röthemeyer and F. Sommer, *Kautschuktechnologie: Werkstoffe - Verarbeitung - Produkte* (Hanser, 2001).

38. S. Ramarad, M. Khalid, C. Ratnam, A. L. Chuah, and W. Rashmi, "Waste Tire Rubber in Polymer Blends: A Review on the Evolution, Properties and Future," *Progress in Materials Science* 72 (2015): 100–140.

39. P. T. Callaghan and A. M. Gil, "1 H NMR Spectroscopy of Polymers Under Shear and Extensional Flow," *Rheologica Acta* 38, no. 6 (1999): 528–536.

40. C. A. Cáceres and S. V. Canevarolo, "Calculating the Chain Scission Distribution Function (CSDF) Using the Concentration Method," *Polymer Degradation and Stability* 86, no. 3 (2004): 437–444.

41. A. Colbourne, T. Blythe, R. Barua, et al., "Validation of a Low Field Rheo-NMR Instrument and Application to Shear-Induced Migration of Suspended Non-Colloidal Particles in Couette Flow," *Journal of Magnetic Resonance* 286 (2018): 30–35.

42. C. Schmidt, "Rheo-NMR Spectroscopy," in *Modern Magnetic Resonance*, ed. G. A. Webb (Springer, 2006), 1515–1521.

43. B. Wiesner, B. Kohn, M. Mende, and U. Scheler, "Polymer Chain Mobility Under Shear—A Rheo-NMR Investigation," *Polymers* 10, no. 11 (2018): 1231.

44. Y. Xiong, Z. Wu, L. Wu, C. Li, and W. Chen, "Rheo-NMR: A Versatile Hyphenated Technique for Capturing Molecular Dynamics and Structure Under Flow," *Magnetic Resonance Letters* 4, no. 1 (2024): 100088.

45. H. Y. Carr and E. M. Purcell, "Effects of Diffusion on Free Precession in Nuclear Magnetic Resonance Experiments," *Physical Review* 94, no. 3 (1954): 630–638.

46. S. Meiboom and D. Gill, "Modified Spin-Echo Method for Measuring Nuclear Relaxation Times," *Review of Scientific Instruments* 29, no. 8 (1958): 688–691.

47. B. Suh, F. Borsa, and D. Torgeson, "Use of an Alternating-Phase CPMG Sequence to Avoid Spin-Locking Effects in T2 Measurements in Solids," *Journal of Magnetic Resonance, Series A* 110, no. 1 (1994): 58–61.

48. V. Litvinov and Y. Men, "Time-Domain NMR in Polyolefin Research," *Polymer* 256 (2022): 125205.

49. A. K. Whittaker, T. Bremner, and F. O. Zelaya, "The Effect of Field Inhomogeneities and Molecular Diffusion on the NMR Transverse Relaxation Behaviour of Polymer Melts," *Polymer* 36, no. 11 (1995): 2159–2164.

50. J. Addad, "NMR and Fractal Properties of Polymeric Liquids and Gels," *Progress in Nuclear Magnetic Resonance Spectroscopy* 25, no. 1–3 (1993): 1–316.

51. M. G. Brereton, "NMR Transverse Relaxation Function Calculated for Constrained Polymer Chains: Application to Entanglements and Networks," *Macromolecules* 23, no. 4 (1990): 1119–1131.

52. C. Liu, J. He, E. v. Ruymbeke, R. Keunings, and C. Bailly, "Evaluation of Different Methods for the Determination of the Plateau Modulus and the Entanglement Molecular Weight," *Polymer* 47, no. 13 (2006): 4461–4479.

53. G. Simon, K. Baumann, and W. Gronski, "Mc Determination and Molecular Dynamics in Crosslinked 1,4-Cis-Polybutadiene: A Comparison of Transversal Proton and Deuterium NMR Relaxation," *Macromolecules* 25, no. 14 (1992): 3624–3628.

54. R. K. Harris, B. J. Say, and S. Ng, "Proton NMR Studies of Molecular-Level Mobility in Vulcanised and Epoxidised Natural Rubber," *Polymer International* 40, no. 1 (1996): 63–71.

55. J. W. ten Brinke, V. M. Litvinov, J. E. G. J. Wijnhoven, and J. W. M. Noordermeer, "Interactions of Stöber Silica With Natural Rubber Under the Influence of Coupling Agents, Studied by $^{1}$H NMR $T2$ Relaxation Analysis," *Macromolecules* 35, no. 27 (2002): 10026–10037.

56. S. Frosch, "Diffusion Processes in Ground Rubber Containing Compounds" (PhD, University of Twente, 2024).

57. N. W. Radebe, C. Fengler, C. O. Klein, R. Figuli, and M. Wilhelm, "Rheo-IR: A Combined Setup for Correlating Chemical Changes via FTIR Spectroscopy and Rheological Properties in a Strain-Controlled Rheometer," *Journal of Rheology* 65, no. 4 (2021): 681–693.



10974628, 0, Downloaded from https://onlinelibrary.wiley.com/doi/10.1002/app.71322 by Karlsruher Institut Fur Technologie, Wiley Online Library on [28/08/2026]. See the Terms and Conditions (https://onlinelibrary.wiley.com/terms-and-conditions) on Wiley Online Library for rules of use; OA articles are governed by the applicable Creative Commons License